Published in final edited form as:
Stem Cells. 2007 August ; 25(8): 1995–2005. doi:10.1634/stemcells.2006-0677.

Human Amniotic Epithelial Cells as Novel Feeder Layers for Promoting Ex Vivo Expansion of Limbal Epithelial Progenitor Cells

Ying Ting Chen[a,b,c], **Wei Li**[a], **Yasutaka Hayashida**[a], **Hua He**[a], **Szu Yu Chen**[a], **David Y. Tseng**[a], **Ahmad Kheirkhah**[a], and **Scheffer C. G. Tseng**[a]

[a]TissueTech, Inc. and Ocular Surface Center, Miami, Florida, USA

[b]Department of Ophthalmology, College of Medicine, National Cheng Kung University, Tainan, Taiwan

[c]Institute of Clinical Medicine, College of Medicine, National Cheng Kung University, Tainan, Taiwan

Abstract

Human amniotic epithelial cells (HAECs) are a unique embryonic cell source that potentially can be used as feeder layers for expanding different types of stem cells. *In vivo*, HAECs uniformly expressed pan-cytokeratins (pan-CK) and heterogeneously expressed vimentin (Vim). The two phenotypes expressing either pan-CK (+)/Vim(+) or pan-CK(+)/Vim(−) were maintained in serum-free media with high calcium. In contrast, all HAECs became pan-CK (+)/Vim(+) in serum-containing media, which also promoted HAEC proliferation for at least 8 passages especially supplemented with EGF and insulin. Mitomycin C-arrested HAEC feeder layers were more effective in promoting clonal growth of human limbal epithelial progenitors than conventional 3T3 murine feeder layers. Cells in HAEC-supported clones were uniformly smaller, sustained more proliferation, and expressed less CK12 and connexin 43, but higher levels of stem cell-associated markers such as p63, Musashi-1 and ABCG2 than those of 3T3-supported clones. Subculturing of clonally expanded limbal progenitors from HAEC feeder layers, but not from 3T3 feeder layers, gave rise to uniformly p63-positive epithelial progenitor cells as well as nestin-positive neuronal-like progenitors. Collectively, these results indicated that HAECs can be used as a human feeder layer equivalent for more effective *ex vivo* expansion of adult epithelial stem cells from the human limbus.

Keywords

ABCG2; amniotic membrane; amniotic epithelial cells; ex vivo expansion; feeder layers; connexin 43 cytokeratins; K12; limbus; Musashi-1; neuronal progenitors; plasticity; progenitor cells; p63; stem cells

Introduction

The maintenance of a healthy corneal epithelium and the repair of a damaged corneal surface are achieved by a unique group of stem cells residing in the limbal basal epithelium

Corresponding Author: Scheffer C. G. Tseng, MD, PhD, Ocular Surface Center, 7000 SW 97 Avenue, Suite 213, Miami, FL 33173, USA, TEL: (305) 274-1299, FAX: (305) 274-1297, stseng@ocularsurface.com.

[1]. *Ex vivo* expansion of autologous limbal epithelial stem cells from a small limbal biopsy taken from the donor's healthy eye has been used as a new surgical graft to treat corneas manifesting unilateral total limbal stem cell deficiency [2]. The success of this new surgical strategy depends on effective *ex vivo* expansion on co-cultured murine 3T3 fibroblast feeder layers, a method first introduced by Rheinwald and Green in 1975 [3] by suppressing 3T3 fibroblast growth while maintaining their viability by either beta-irradiation or mitomycin C. Indeed, mitomycin C-treated 3T3 fibroblast feeder layers have been used to cultivate epithelial cells from human limbus [4], conjunctiva [5], and oral mucosa [6].

One potential biohazard of using murine fibroblast feeder layers for human transplantation is the transmission of murine diseases. Moreover, it has also been reported that human embryonic stem cells cultured on mouse feeder layers generate an immunogenic non-human sialic acid [7]. Therefore, there is an increasing need to substitute 3T3 fibroblast feeder layers with a human equivalent to avoid xenotoxicity. We hypothesize that human amniotic epithelial cells (HAECs) may be an ideal candidate. This hypothesis is suggested by our prior reports showing that a limbal epithelial phenotype is preserved when limbal explants are grown on an intact amniotic membrane that retains a devitalized amniotic epithelium [8]. In contrast, the resultant epithelium turns into a corneal epithelial phenotype when limbal explants are grown on an epithelially-denuded amniotic membrane [8]. These findings highlight the importance of HAECs in providing a needed support for limbal epithelial stem cells.

From the tissue engineering viewpoint, a higher number of passages are more desirable, facilitating generation of sufficient numbers of HAECs for the preparation of feeder layers. Unfortunately, culturing conditions regarding HAECs have not been fully optimized, nor has the *in vitro* HAEC phenotype been well defined. HAEC cultures reported thus far are limited to early passages (either P0 or P1) [9–12]. In this study, we promoted proliferation of HAECs with dual expression of cytokeratins (CKs) and vimentin (Vim) by increasing extracellular calcium concentrations ($[Ca^{2+}]$) and addition of fetal bovine serum (FBS), and subcultured HAECs for at least 8 passages in SHEM medium with growth factors. Feeder layers prepared from such expanded HAECs were more effective than 3T3 fibroblast feeder layers in expanding undifferentiated human limbal epithelial progenitors and promoting their plasticity in exhibiting a neuron-like phenotype. Perspectives on tissue engineering of HAEC feeder layers are further discussed.

Materials and Methods

Human tissue was handled according to the Declaration of Helsinki. Fresh full-term human placentas were procured from healthy mothers after elective Caesarean approved by the institutional review board of the Baptist Hospital in Miami. Corneoscleral tissues from human donor eyes were obtained from the Florida Lions Eye Bank (Miami, FL) immediately after corneal transplantation. Mouse NIH 3T3 fibroblasts (ATCC CRL-1658) were from American Type Culture Collection (Manassas, VA). Materials for cell cultures were listed in Table 1 of Supplementary Information. All the antibodies used for immunofluorescence staining, immunohistochemistry and Western blotting are listed in Table 2 of Supplementary Information.

Isolation of HAECs

Human placentas were washed twice in HBSS for 5 min each to remove the blood. An intact layer of the amnion was mechanically peeled off from the chorion, cut into pieces of approximately 5 × 5 cm^2, and rinsed in HBSS for another 5 min. The amnion was then incubated with 10 mg/ml Dispase II in KSFM at 37 °C for 15 min to generate a loose single layer of the amniotic epithelium, which was then stripped off with jeweler's forceps from

the underlying stroma. Isolated epithelial sheets were further digested with 0.25% Trypsin/1mM EDTA at 37 °C for 15 min; dissociated cells were collected after centrifugation at 2,000 rpm for 5 min. Cell viability was determined by exclusion of trypan blue dye and counted with a hemocytometer.

Cell Cultures in Different Media

Single HAECs isolated from the amnion were plated on 100-mm-diameter culture dish at a density of 1.27×10^4 cells per cm^2 in 9 different media made of KSFM, DMEM/F12, or SHEM. For both KSFM and DMEM/F12, additional modifications were made by adding calcium chloride and/or FBS (for more details see Table 3 in Supplementary Information). All experiments were performed in triplicate per condition. After reaching subconfluence, cells were digested with Trypsin/EDTA and subcultured at a 1:3 split in a given medium.

MTT Cell Proliferation Assay for HAECs

In order to study how cell proliferation might be affected by different media, the first passage of HAECs cultured in SHEM was subsequently subcultured in each of the above-mentioned 9 media and subjected to MTT assay, which is based on the cleavage of yellow tetrazolium salt MTT to purple formazan crystals by metabolically-active cells [12]. After cells were incubated for 4 h, formation of formazan dye in the microtiterplate was spectrophotometrically quantified with an ELISA plate reader set at 570 nm. Experiments were conducted using 5 samples per condition.

Clonal Growth and Cell Proliferation

In order to examine whether HAECs could support clonal growth of human limbal progenitor cells, a clonal assay was performed using a method reported earlier [3] and modified by us for limbal epithelial cells [13]. In brief, NIH 3T3 fibroblasts grown in DMEM containing 10% new borne calf serum at 80% subconfluence and the 8^{th} passage of HAECs grown in SHEM were treated with 4 μg/ml mitomycin C for 2 h and then trypsinized and plated at a density of 2×10^4 cells/cm^2. Human limbal epithelial sheets were isolated directly from corneoscleral rims obtained immediately after penetrating keratoplasty based on our modified digestion method using 10 mg/ml Dispase II in SHEM at 4°C for 16 h [14]. Isolated limbal epithelial sheets were rendered into single cells by digestion with 0.05% trypsin/0.53 mM EDTA at 37 ºC for 15 min, and seeded in triplicate at a density of 50 cells/cm^2 (500 cells/well) on either HAEC or 3T3 fibroblast feeder layers in six-well culture plates containing SHEM. Cultures were incubated at 37ºC under 5% CO_2 and 95% humidity, and the medium was changed every 2–3 days. Colonies were counted at Day 6 (D6) and D10, followed by fixation in cold methanol at D10 or D14, stained with crystal violet dye, and photographed. The colony-forming efficiency (CFE) was calculated as the number of colonies per well divided by 500 (i.e., the total seeded cells per well). Cell sizes of colonies were determined by an imaging software using AlphaImage 2200 (version 3.2.1, AlphaInnotech, San Leandro, CA) by selecting 3 clones of similar sizes (at least 2.5 mm in diameter) from each feeder layer. Because the cell size in HAEC-supported clones was homogeneous while that of 3T3-supported clones was heterogeneous, 10 randomly chosen fields at 400x magnification were taken for each selected HAEC-supported clone to be compared with 5 randomly chosen fields taken from the periphery and the center of each 3T3-supported clone, respectively, for calculating clonal cell grown on those two feeder layers. On D10, D14 and D18, three plates of limbal clonal cultures from each feeder system were terminated for immunostaining of Ki67 nuclear expression, and the percentage of positive cells in each clone was defined as proliferation index and compared in these two feeder layers using the same sampling method as described above.

Reverse Transcription and Relatively Quantitative Real-Time PCR

Total RNA was extracted from limbal epithelial clones from each feeder system in a 35-mm dish culture on D10 using RNeasy Mini RNA isolation kit (Qiagen, Germany). Total RNA was eluted from the mini columns with 30 μl of RNase-free water. The amount of total RNA isolation was quantified by optical density at 260nm (OD_{260}). Starting from 1 μg of total RNA, 80 μl of cDNA was synthesized using Tagman Reverse Transcription Reagent (Applied Biosystems, Foster City, CA) which contains Oligo $d(T)_{16}$, RNase inhibitor, deoxyNTPs mixture and MultiScribe reverse transcriptase. The reaction was performed for 10 min at 25°C, for 60 min at 37°C, and for 5 min at 95°C. cDNA was then stored at −20 °C until use. To compare the relative abundance of transcripts expressed, a TagMan Probe fluorogenic 5′nuclease chemistry-based real-time PCR was used to make relative quantitation with ABI Prism 7300 Real Time PCR System (Applied Biosystems, Fort City, CA). The real-time PCR reaction mixture was prepared in a 20 μl solution, containing cDNA, TagMan forward and reverse primers, probes in TagMan Gene Expression Assay Mix, and TagMan Universal PCR Master Mix (Applied Biosystems, Fort City, CA). Five out of six sets of primers used in the study crossed two exons to avoid non-specific DNA amplication. All the TagMan Gene Expression Assays with probe sequences used were listed in Table 4 of Supplementary Information. The real-time PCR was performed using thermal cycling conditions at 50°C for 2 min, at 95°C for 10 min as initial steps, followed by 40 cycles of 15 sec at 95°C and 1 min at 60°C for amplification. All assays were performed in three different limbal donors and each in triplicate, and with a nontemplate control to evaluate potential DNA contamination. The results of relatively quantitative real-time PCR were analyzed by the comparative threshold cycle method and normalized by GAPDH as an internal control. To confirm the specificity of PCR amplification, the end-product of PCR was subject to DNA electrophoresis to determine the length of amplicons.

Statistical Analysis

Summary data of cell sizes, MTT, rates of positive immunostaining and relative fold of real-time PCR were reported as means ± SD and compared using the Student's unpaired t-test of Microsoft Excel (2003/XP version). Test results were reported as two-tailed p values, where $p < 0.05$ was considered statistically significant.

Results

Characterization of HAEC Phenotype *In Vivo*

As a baseline, we first determined the epithelial phenotype *in vivo*. H & E section (Fig. 1A1) revealed that the amnion was composed of a single epithelial layer and an avascular stroma, which contained mesenchymal cells. In line with previous studies [9;15], our baseline immunostaining characterization showed that *in vivo* HAECs indeed did not express CK4 and CK5/6, but expressed CK8, CK14, CK17, CK18 and CK19 throughout the entire epithelium (Fig. 1A1–8). Vimentin (Vim), a mesenchymal marker, was expressed by all stromal cells, and also by clusters of HAECs (Fig. 1A11). This heterogeneous expression of Vim in HAECs was further confirmed by double immunostaining to pan-CK and Vim (Fig. 1A12). Nearly all HAECs were devoid of any labeling to Ki67, an indicator of proliferation (Fig. 1A9), suggesting that HAECs of the full term placenta were mitotically quiescent.

Characterization of HAEC Phenotype *In Vitro*

HAECs immediately harvested from the fresh placenta could be cultured in all 9 different media (see Table 3 in Supplementary Information). In serum-free, calcium-free or low calcium media (Condition 1, KSFM and Condition 5, DMEM/F12), HAECs became small and round with a high nucleus-to-cytoplasm (N/C) ratio, and were scattered around as single

cells (Fig. 1B1). The proliferation rate indicated by the number of Ki67-positive cells was extremely low (Fig. 1B2). Interestingly, some cells gradually lost expression of pan-CK over time and turned into Vim-expressing cells (Fig. 1B5, open arrow). The rest of cells either showed a pan-CK(+)/Vim(+) (Fig. 1B5, solid arrow head), or a pan-CK(−)/Vim(−) phenotype (Fig. 1B5, asterisks). In serum-free, high-calcium media (Condition 2, KSFM and Condition 6, DMEM/F12), HAECs remained small and round, and had a high N/C ratio, but gathered to form clusters or small sheets (Fig. 1C1). Cell proliferation was still largely halted (Fig. 1C2). Intriguingly, HAECs maintained either pan-CK(+)/Vim(−) cells (Fig. 1C5, arrow) or pan-CK(+)/Vim(+) cells (Fig. 1C5, solid arrow head), resembling what was observed *in vivo* (Fig. 1A12). In serum-containing but low-calcium media (Condition 3, KSFM and Condition 7, DMEM/F12), HAECs changed to a cobble-stone-like shape with a low N/C ratio, and formed a sheet with obviously discernible intercellular junctions (Fig. 1D1). There were numerous Ki67 positive cells (Fig. 1D2). Most cells co-expressed pan-CK and Vim (Fig. 1D5, solid arrow head) while a minority showed a pan-CK-only phenotype (Fig. 1D5, arrow). A fibrillar staining pattern was noted in plethora of cells, while a few cells had a unique perinuclear “Vim ring” (Fig. 1D5, open arrow head). Finally, when $[Ca^{2+}]$ was increased to 1.08 mM in serum-containing media (Condition 4, KSFM; Condition 8, DMEM/F12; and Condition 9, SHEM), the cell morphology and differentiation remained similar to that described above in serum-containing low calcium media (not shown). MTT proliferation assay was used to compare the proliferative activity of HAECs in these 9 different media (Fig. 2E). Similar to Ki67 staining patterns, adding FBS significantly promoted cell proliferation when compared to their serum-free counterparts. Increase of $[Ca^{2+}]$ in either KSFM or DMEM/F12 increased cell proliferation to a lesser extent. Interestingly, SHEM which contains 5% FBS and other growth supplements yielded the highest proliferation of HAECs ($p = 0.011$ versus condition 4 and $p < 0.01$ versus other 7 conditions, n = 5).

To confirm if SHEM is indeed the best culture medium to support the growth of HAECs *in vitro*, we further compared the maximum of cell passage numbers achieved by each culturing medium. In serum-free media, HAECs did not reach confluence by the end of one month at Passage 0 (P0). When $[Ca^{2+}]$ was increased to 1.05 mM), cell proliferation improved but not enough to be cultured beyond P2. The addition of FBS in low-calcium or calcium-free media or in high-calcium media did not significantly further improve the maximal passage numbers, and cells reached senescence by P3 or P4. Only in SHEM could HAECs actively proliferate, reach confluence in 3 days at 1:3 split, and maintain an epithelial shape for at least P8.

Therefore, we would like to further characterize their proliferation rate and phenotypes from low to high passages in SHEM. At P0, HAECs lost the *in vivo* expression of CK18 (Fig. 2A), while continued to show positive immunoreactivity to pan-CK (Fig. 2B). At that time, a substantial number of HAECs showed positive nuclear staining of Ki67 (Fig. 2C). At P1, HAECs regained expression of CK18 although the staining intensity was weaker than their *in vivo* counterpart (Fig. 2D). Their positive immunoreactivity to pan-CK was stronger than P0 (Fig. 2E), while staining to Ki67 did not change (Fig. 2F). At P4, HAECs had a more intense CK18 expression (Fig. 2G) and fibrillar pan-CK staining (Fig. 2H), and the number of Ki67 positive nuclei reached its peak (Fig. 2I) when compared to P0, P1, and P7. Strong cytoplasmic staining to Pan-CK and CK18 was found in every cell at P7 (Fig. 2K and 2J, respectively). Consistent with the immunostaining results, Western blot analysis showed an increase of CK18 from low passages to high passages. Expression of Vim was slightly decreased in P1 cultures but also eventually much increased at P7 cultures (Fig. 2M). Taken together, these data indicated that HAECs could be successively propagated in SHEM and maintained a phenotype with co-expression of both epithelial and mesenchymal intermediate filaments.

Limbal Clonal Growth Were Better Supported by HAEC than 3T3 Feeder Layers

With HAECs successfully expanded to P8 with sufficient numbers, we then compared the clonal growth of limbal progenitor cells supported by mitomycin C-treated HAEC feeder layers to that supported by mitomycin C-treated 3T3 feeder layers. As shown in Figure 3, limbal clones grown on 3T3 feeder layers emerged as early as D3, but those on HAEC feeder layers did slower, i.e., after at least 5 days. HAEC-supported clones were fewer and smaller than 3T3-supported clones (Fig. 3A). The border of limbal clones on 3T3 feeder layers was smooth presumably because 3T3 fibroblasts were pushed by the expanding limbal epithelial cells. Interestingly, the border of limbal clones on HAEC was irregular because the entire clone was growing on the top of their underlying feeder cells (not shown). As shown in Figure 3B, the CFE on the HAEC feeder layer was 1.1 ± 0.4 % on D6 and 2.4 ± 0.7 % on D10, which were significantly less than 7.2 ± 1.2 % ($p = 0.007$, n = 3) and 11.1 ± 2.1 % ($p = 0.011$, n = 3) on their 3T3 counterparts, respectively. Under low magnification, HAEC-supported clones were uniformly compacted with small cells (Fig. 3C, F). In contrast, cells in the center of 3T3-supported clones had an increased cell size and were squamous (Fig. 3D, 3G and 3H). Indeed, the average cell size for HAEC-supported clones was 19.8 ± 2.2 μm, which was much smaller than 24.4 ± 2.0 μm of the periphery ($p = 0.028$, n = 3) and 44.2 ± 2.2 μm of the center ($p = 0.017$, n = 3) of 3T3-supported clones (Fig. 3E).

The above cell size change was correlated with the cell proliferation pattern. Almost every cell in HAEC-supported clones showed positive Ki67 nuclear staining on D10 (Fig. 4A), and continued to be sustained on D14 (Fig. 4B) and D18 (Fig. 4C). In contrast, cells on 3T3-supported clones initially showed high proliferation on D10 (Fig. 4D) but quickly dropped on D14 (Fig. 4E) and became almost undetectable on D18 (data not shown). Therefore, a homogenous pattern of Ki67 expression was observed in the entire clone throughout all time points on HAECs (Fig. 4A–C, 4F1–4). In contrast, Ki67 expression faded away from the center as early as D10 (Fig. 4D, 4F6) and the number of Ki67 negative cells increased in 3T3-supported clones thereafter (Fig. 4E, 4F7–8). These differences could also be revealed by calculating the percentage of Ki67 positive cells over time (Fig. 4G). These results collectively indicated that sustained high cell proliferation was uniformly maintained in HAEC-supported clones, but lost in the center of 3T3-supported counterparts during the exponential clonal growth.

We then would like to know whether the above changes were correlated with cellular differentiation. As expected, CK12 was not expressed by the amniotic epithelium (Fig. 5A), but expressed by human limbal suprabasal cells [16;17] (Fig. 5C). Except for few single cells in the center of the clone, expression of CK12 was totally negative in HAEC-supported clones (Fig. 5D). On the contrary, many cells in the center of 3T3-supported clones vividly expressed CK12 (Fig. 5E). The percentage of CK12-postive cells, indicative of the extent of corneal epithelial differentiation, was significantly higher in 3T3-supported clones than that in HAEC-supported clones (14.8 ± 5.0 % versus 1.8 ± 1.6 %) ($p = 0.019$, n = 3) (Fig. 5B). As expected, we also noted a punctate staining pattern of connexin 43 at intercellular junctions in the suprabasal layers of the human limbal epithelium [18;19] (Fig. 5F). Interestingly, cells in HAEC-supported clones were entirely negative to the connexin 43 staining (Fig. 5G). In contrast, some cells from the mid-periphery and the center of 3T3-supported clones revealed positive Cx43 staining at intercellular junctions (Fig. 5H). Relative quantitative real-time PCR showed CK12 transcript expression by HAEC-supported clones was significantly decreased to 0.27-fold of that of 3T3-supported clones (ranging from 0.09 to 0.571-fold in 3 different limbal donors, $P<0.01$ compared to 1-fold), whereas connexin 43 transcript didn't show any significant difference (Fig. 5L).

We then would like to determine whether HAEC-supported clones actually expressed more stem cell-associated markers such as p63, Musashi-1, and ABCG2. Positive nuclear p63

immunostaining was found in nearly all cells of HAEC-supported clones (Fig. 6B). In contrast, positive nuclear p63 staining was relatively restricted to peripheral small cells (Fig. 6C), but not in the center of 3T3-supported clones (Fig. 6D). The percentage of p63-positive cells in HAEC-supported clones was 93.7 ± 4.4 %, which was significantly higher than 63.5 ± 16.3 % in 3T3-supported clones ($p = 0.030$, n = 4) (Fig. 6E). Musashi-1, a neural stem cell marker [22], was found in the nucleus of the subventrical zone of the mouse brain (Fig. 6F inset). In the human limbus, strong nuclear staining of Musashi-1 was found in basal epithelial cells with a faint staining noted throughout the whole epithelium (Fig. 6F). Nuclear expression of Musashi-1 was found in most cells of HAEC-supported clones (Fig. 6G). In contrast, there was a gradient of positive nuclear staining from the periphery (Fig 6H) to the center (Fig 6I) of 3T3-supported clones. The percentage of Musashi-1-positive cells in HAEC-supported clones was 68.3 ± 2.6 %, which was significantly higher than 26.8 ± 15.8 % in 3T3-supported clones ($p = 0.012$, n = 4) (Fig. 6J). Expression of ATP-binding cassette subfamily G2 (ABCG2) plasma membrane transporter is highly conserved in primitive stem cells from a variety of tissue sources [23]. Consistent with what was reported by Watanabe et al [24], we found that the expression of ABCG2 was predominantly confined to limbal basal epithelial cells (Fig. 6K). In HAEC-supported clones, the majority of cells were positively stained to ABCG2, forming patches intermixed with few negative cells throughout the entire clone (Fig. 6L). In contrast, ABCG2 was mainly expressed in clusters of small cells in the periphery of 3T3-supported clones (Fig. 6M) but not in the center of the clone (Fig. 6N). The percentage of ABCG2-positive cells in HAEC-supported clones was 87.5 ± 6.3 %, which was significantly higher than 54.9 ± 19.1 % in 3T3-supported clones ($p = 0.036$, n = 4) (Fig. 6O). Relative quantitative real-time PCR also confirmed that the level of p63, Musashi-1, and ABCG2 transcript in HAEC-supported clones were 3.9-fold (ranging from 3.4 to 4.7), 12.6-fold (ranging from 9.3 to 18.0), and 34.1-fold (ranging from 23.0 to 42.0) higher than that of 3T3-supported clones, respectively (Fig. 6P, each from 3 different donors). Taken together, these data indicated that HAEC-supported clones expressed significantly more stem cell-associated markers than 3T3-supported clones, indicative of preservation of more epithelial stem cells.

Limbal Clones Subcultured on HAEC Feeder Layers Exhibited Sustained Clonogeneity and Neuron-like Characteristics

We then wondered if HAEC-supported limbal clones could be subcultured, and if so whether they exhibited more plasticity. When HAEC-supported limbal clones were subcultured on HAEC feeder layers, we observed two morphologically distinct clones. One was the expected epithelial clone (Fig. 7A), which did not expressed CK12 (Fig. 7B), but expressed p63 in nearly all nuclei (Fig. 7C). The other clone contained neuron-like cells (Fig. 7D), which expressed neurofilament 200 in their dendritic cytoplasmic processes (Fig. 7E). In addition, there were also small and less elongated cells forming a filamentous “nest” [25] that expressed nestin, regarded as a neuroepithelial stem cell marker [26], in the perinuclear cytoplasm (Fig. 7F). In contrast, when 3T3-supported limbal clones were subcultured on 3T3 feeder layers, we only observed one type of epithelial clone (Fig. 7G), which also did not expressed CK12 (Fig. 7H), but only few cells in the periphery still expressed p63 in the nucleus (Fig. 7I). Collectively, these data further indicated that limbal epithelial progenitor cells supported by HAEC feeder layers, attained clonogenicity and exhibited neural characteristics.

Discussion

Adult limbal progenitors normally are mitotically quiescent *in vivo*, but can be activated to proliferate *in vitro*. Without 3T3 fibroblast feeder layers, they quickly differentiate and lose stemness. Even when cocultured with 3T3 fibroblast feeder layers, our study showed that

cells in the center of 3T3-supported clones gradually ceased proliferation, presumably due to the lack of direct contact with 3T3 fibroblasts (Fig. 3). Consequently, they underwent more differentiation as evidenced by larger cell sizes and more expression of CK12 [27, 28] and connexin 43 [18, 19, 29] (Fig. 5), both markers known to be expressed by limbal suprabasal epithelial cells. In contrast, cells in HAEC-supported clones were uniformly small (Fig. 3), a feature known for limbal basal epithelial progenitors [30, 31] and epidermal progenitors [32]. Furthermore, the expression of CK12 in HAEC-supported clones was consistently absent as judged by both immunostaining and real-time PCR data, while that of connexin 43 was absent by immunostaining data but not by real-time PCR data (Fig. 5). The latter discrepancy might be caused by different donors or because total mRNAs collected from the entire clone might not reveal patchy positive immunostaining to connexin 43 in the mid-periphery to center of 3T3-supported clones. Small epithelial progenitors expressing less cornea-specific CK12 and connexin 43 have also preferentially been expanded on an HAEC-containing intact amniotic membrane but not on an HAEC-denuded amniotic membrane [8, 33]. We speculate that a small cell size and the lack of differentiation in the entire HAEC-supported clone might be achieved partly by its uniform contact with growth-arrested HAECs.

From the outset, 3T3-supported clones had a higher colony-forming efficiency than HAEC-supported clones (Fig. 3). This seemingly advantageous result was negated by the lack of preservation of an undifferentiated state as mentioned above and furthermore by the lack of uniform Ki67 nuclear staining during clonal growth. In contrast, both features were maintained by HAEC-supported clones (Fig. 4). Limbal epithelial progenitors sorted as the side population by flow cytometry according to the efflux of Hoechst 33342 have a lower colony-forming efficiency than that of non-fractionated total limbal cells on 3T3 fibroblast feeder layers [34, 35]. Therefore, future studies are needed to resolve whether 3T3 fibroblast feeder layers actually expand additional transient amplifying cells.

Cumulating evidence suggests that rather than any single marker, a panel of multiple stem cell-associated markers is expressed as a signature of various adult stem cells. Besides a small cell size and an undifferentiated status, HAEC-supported limbal clones also expressed significantly high levels of such stem cell-associated markers as p63, Musashi-1 and ABCG2 at the protein and transcript levels (Fig. 6). p63 plays a key role in ectodermal differentiation during development and the maintenance of stratified epithelial progenitor cells [36]. Although p63 was originally regarded as a putative stem cell marker for limbal progenitors [20], it was recently found also being expressed by the corneal basal epithelium [37]. ABCG2, an ATP binding cassette transporter encoded by *Bcrp1*, is responsible for the side population for many types of stem cells [38]. Although ABCG2 is expressed by limbal basal epithelial progenitors [24], it is also expressed by limbal stromal cells [39] and by Langerhan's cells residing in the limbal basal layer [40]. Musashi-1, a putative neural stem cell marker, is an RNA-binding protein involved in asymmetric divisions of sensory organ precursor cells in Drosophila [41], and plays an important role in the maintenance of stem cells and in the activation of Notch-mediated stem cell signaling [42, 43]. Our study is the first showing that the ectodermally derived stem cell-containing limbal epithelium also expressed Musashi-1 (Fig. 6E), which together with p63 and ABCG2 may serve as a signature of stem cell marker for defining limbal epithelial progenitor cells in the future.

Although the exact mechanism to explain how epithelial stem cells are supported by feeder layers remains elusive, most feeder layers capable of supporting stem cells are derived from the mesenchyme [44–46]. Besides expression of a number of CKs, some HAECs *in vivo* also co-expressed Vim (Fig. 1). Dual expression of CKs and Vim was observed in HAECs *in vitro* (Fig. 2). In serum-free, high calcium media, HAECs expressed either Pan-CK(+)/Vim(+) or Pan-CK(+)/Vim(−), but addition of FBS rendered all cells to Pan-CK(+)/Vim(+),

consistent with what has been previously reported [47]. However, inclusion of additional EGF, insulin and other supplements in SHEM dramatically helped to expand HAECs to at least P8 (Fig. 3), while maintaining their dual expression of CKs and Vim. The fact that HAECs may adopt a mesenchymal phenotype is also supported by their multipotency in generating the epidermis, hair follicles (ectoderm) and cardiomyocytes (mesoderm) when transplanted in mice [11, 48]. Furthermore, cultured perivascular stromal cells of the umbilical cord, another close kinship of the amniotic membranes, also coexpress CKs and Vim [25]. We thus speculate that increased Vim expression by HAECs in SHEM may have promoted their capacity of serving as feeder layers. Interestingly, HAECs can be used as feeder layers to support the growth of primate embryonic stem cells without differentiation [9].

Intriguingly, most likely due to increased preservation of stem cell characteristics, HAEC-supported limbal clones were conferred with more plasticity. In the current study, upon subculturing, both feeder layers produced epithelial clones, but cells in the center of 3T3-supported clones already lost their progenitor status as shown by the loss of nuclear expression of p63 (Fig. 7), similar to what has been reported in limbal explant cultures without feeder layers [37]. Besides epithelial clones, HAEC-supported clones also revealed morphologically distinct dendritic cells with neural phenotypes (Fig. 7). The reason why limbal progenitors display some neural characteristics on HAEC feeder layers may be related to neurotrophic factors secreted by HAEC [49] and/or the common embryonic neuroepithelial origin shared between neurons and limbus. Further investigation is needed to determine whether this finding represents neural transdifferentiation.

In summary, our study has demonstrated that HAECs can be subcultured in SHEM to a sufficient number for use as a non-murine feeder layer to expand human limbal epithelial progenitors more effectively than traditional 3T3 fibroblasts. Furthermore, HAEC feeder layers can promote limbal progenitor's plasticity to adopt neural-like differentiation. Further studies on the growth-supporting capability of HAECs for ex vivo expansion of other types of adult stem cells may unravel their usefulness as a human feeder cell source in regenerative medicine.

Supplementary Material

Refer to Web version on PubMed Central for supplementary material.

Acknowledgments

This study was supported by EY06819 and EY015735 grants (SCGT) from National Eye Institute, National Institute of Health, Bethesda, MD, and research grants from TissueTech, Inc. and Y-T C is a recipient of Joe Swiger and Eye Foundation of American Fellowship from Ocular Surface Research and Education Foundation, Miami, FL.

References

1. Lavker RM, Tseng SC, Sun TT. Corneal epithelial stem cells at the limbus: looking at some old problems from a new angle. Exp Eye Res. 2004; 78:433–446. [PubMed: 15106923]
2. Pellegrini G, Traverso CE, Franzi AT, Zingirian M, Cancedda R, De Luca M. Long-term restoration of damaged corneal surface with autologous cultivated corneal epithelium. Lancet. 1997; 349:990–993. [PubMed: 9100626]
3. Rheinwald JG, Green H. Serial cultivation of strains of human epidermal keratinocytes: the formation of keratinizing colonies from single cells. Cell. 1975; 6:331–337. [PubMed: 1052771]
4. Lindberg K, Brown ME, Chaves HV, Kenyon KR, Rheinwald JG. In vitro preparation of human ocular surface epithelial cells for transplantation. Invest Ophthalmol Vis Sci. 1993; 34:2672–2679. [PubMed: 8344790]

5. Wei Z-G, Wu R-L, Lavker RM, Sun T-T. In vitro growth and differentiation of rabbit bulbar, fornix, and palpebral conjunctival epithelia. Implication on conjunctival epithelial transdifferentiation and stem cells. Invest Ophthalmol Vis Sci. 1993; 34:1814–1828. [PubMed: 8473120]
6. Nishida K, Yamato M, Hayashida Y, Watanabe K, Yamamoto K, Adachi E, Nagai S, Kikuchi A, Maeda N, Watanabe H, Okano T, Tano Y. Corneal reconstruction with tissue-engineered cell sheets composed of autologous oral mucosal epithelium. N Engl J Med. 2004; 351:1187–1196. [PubMed: 15371576]
7. Martin MJ, Muotri A, Gage F, Varki A. Human embryonic stem cells express an immunogenic nonhuman sialic acid. Nat Med. 2005; 11:228–232. [PubMed: 15685172]
8. Grueterich M, Espana E, Tseng SC. Connexin 43 expression and proliferation of human limbal epithelium on intact and denuded amniotic membrane. Invest Ophthalmol Vis Sci. 2002; 43:63–71. [PubMed: 11773014]
9. Miyamoto K, Hayashi K, Suzuki T, Ichihara S, Yamada T, Kano Y, Yamabe T, Ito Y. Human placenta feeder layers support undifferentiated growth of primate embryonic stem cells. Stem Cells. 2004; 22:433–440. [PubMed: 15277690]
10. Sakuragawa N, Thangavel R, Mizuguchi M, Hirasawa M, Kamo I. Expression of markers for both neuronal and glial cells in human amniotic epithelial cells. Neurosci Lett. 1996; 209:9–12. [PubMed: 8734897]
11. Miki T, Lehmann T, Cai H, Stolz DB, Strom SC. Stem cell characteristics of amniotic epithelial cells. Stem Cells. 2005; 23:1549–1559. [PubMed: 16081662]
12. Kamiya K, Wang M, Uchida S, Amano S, Oshika T, Sakuragawa N, Hori J. Topical application of culture supernatant from human amniotic epithelial cells suppresses inflammatory reactions in cornea. Exp Eye Res. 2005; 80:671–679. [PubMed: 15862174]
13. Tseng SC, Kruse FE, Merritt J, Li DQ. Comparison between serum-free and fibroblast-cocultured single-cell clonal culture systems: evidence showing that epithelial anti-apoptotic activity is present in 3T3 fibroblast-conditioned media. Curr Eye Res. 1996; 15:973–984. [PubMed: 8921219]
14. Espana EM, Romano AC, Kawakita T, Di Pascuale M, Smiddy R, Tseng SC. Novel enzymatic isolation of an entire viable human limbal epithelial sheet. Invest Ophthalmol Vis Sci. 2003; 44:4275–4281. [PubMed: 14507871]
15. Regauer S, Franke WW, Virtanen I. Intermediate filament cytoskeleton of amnion epithelium and cultured amnion epithelial cells: expression of epidermal cytokeratins in cells of a simple epithelium. J Cell Biol. 1985; 100:997–1009. [PubMed: 2579960]
16. Liu C-Y, Zhu G, Converse R, Kao CW-C, Nakamura H, Tseng SCG, Mui M-M, Seyer J, Justice MJ, Stech ME, Hansen GM, Kao WW-Y. Characterization and chromosomal localization of the cornea-specific murine keratin gene *Krt1.12*. J Biol Chem. 1994; 260:24627–24636. [PubMed: 7523376]
17. Chen WY, Mui MM, Kao WW, Liu CY, Tseng SC. Conjunctival epithelial cells do not transdifferentiate in organotypic cultures: expression of K12 keratin is restricted to corneal epithelium. Curr Eye Res. 1994; 13:765–778. [PubMed: 7531131]
18. Matic M, Petrov IN, Chen S, Wang C, Dimitrijevich SD, Wolosin JM. Stem cells of the corneal epithelium lack connexins and metabolite transfer capacity. Differentiation. 1997; 61:251–260. [PubMed: 9203348]
19. Wolosin JM, Xiong X, Schütte M, Stegman Z, Tieng A. Stem cells and differentiation stages in the limbo-corneal epithelium. Prog Retinal & Eye Res. 2000; 19:223–255.
20. Pellegrini G, Dellambra E, Golisano O, Martinelli E, Fantozzi I, Bondanza S, Ponzin D, McKeon F, De Luca M. p63 identifies keratinocyte stem cells. Proc Natl Acad Sci U S A. 2001; 98:3156–3161. [PubMed: 11248048]
21. Yang A, Schweitzer R, Sun D, Kaghad M, Walker N, Bronson RT, Tabin C, Sharpe A, Caput D, Crum C, McKeon F. p63 is essential for regenerative proliferation in limb, craniofacial and epithelial development. Nature. 1999; 398:714–718. [PubMed: 10227294]
22. Maslov AY, Barone TA, Plunkett RJ, Pruitt SC. Neural stem cell detection, characterization, and age-related changes in the subventricular zone of mice. J Neurosci. 2004; 24:1726–1733. [PubMed: 14973255]

23. Zhou S, Schuetz JD, Bunting KD, Colapietro AM, Sampath J, Morris JJ, Lagutina I, Grosveld GC, Osawa M, Nakauchi H, Sorrentino BP. The ABC transporter Bcrp1/ABCG2 is expressed in a wide variety of stem cells and is a molecular determinant of the side-population phenotype. Nat Med. 2001; 7:1028–1034. [PubMed: 11533706]
24. Watanabe K, Nishida K, Yamato M, Umemoto T, Sumide T, Yamamoto K, Maeda N, Watanabe H, Okano T, Tano Y. Human limbal epithelium contains side population cells expressing the ATP-binding cassette transporter ABCG2. FEBS Lett. 2004; 565:6–10. [PubMed: 15135043]
25. Karahuseyinoglu S, Cinar O, Kilic E, Kara F, Akay GG, Demiralp DO, Tukun A, Uckan D, Can A. Biology of stem cells in human umbilical cord stroma: in situ and in vitro surveys. Stem Cells. 2007; 25:319–331. [PubMed: 17053211]
26. Lendahl U, Zimmerman LB, McKay RD. CNS stem cells express a new class of intermediate filament protein. Cell. 1990; 60:585–595. [PubMed: 1689217]
27. Schermer A, Galvin S, Sun TT. Differentiation-related expression of a major 64K corneal keratin in vivo and in culture suggests limbal location of corneal epithelial stem cells. J Cell Biol. 1986; 103:49–62. [PubMed: 2424919]
28. Chen WYW, Mui M-M, Kao WW-Y, Liu C-Y, Tseng SCG. Conjunctival epithelial cells do not transdifferentiate in organotypic cultures: Expression of K12 keratin is restricted to corneal epithelium. Curr Eye Res. 1994; 13:765–778. [PubMed: 7531131]
29. Chen Z, Evans WH, Pflugfelder SC, Li DQ. Gap junction protein connexin 43 serves as a negative marker for a stem cell-containing population of human limbal epithelial cells. Stem Cells. 2006; 24:1265–1273. [PubMed: 16424398]
30. Romano AC, Espana EM, Yoo SH, Budak MT, Wolosin JM, Tseng SC. Different cell sizes in human limbal and central corneal basal epithelia measured by confocal microscopy and flow cytometry. Invest Ophthalmol Vis Sci. 2003; 44:5125–5129. [PubMed: 14638707]
31. De Paiva CS, Pflugfelder SC, Li DQ. Cell size correlates with phenotype and proliferative capacity in human corneal epithelial cells. Stem Cells. 2006; 24:368–375. [PubMed: 16123387]
32. Barrandon Y, Green H. Cell size as a determinant of the clone-forming ability of human keratinocytes. Proc Natl Acad Sci U S A. 1985; 82:5390–5394. [PubMed: 2410922]
33. Hernandez Galindo EE, Theiss C, Steuhl KP, Meller D. Gap junctional communication in microinjected human limbal and peripheral corneal epithelial cells cultured on intact amniotic membrane. Exp Eye Res. 2003; 76:303–314. [PubMed: 12573659]
34. Budak MT, Alpdogan OS, Zhou M, Lavker RM, Akinci MA, Wolosin JM. Ocular surface epithelia contain ABCG2-dependent side population cells exhibiting features associated with stem cells. J Cell Sci. 2005; 118:1715–1724. [PubMed: 15811951]
35. Umemoto T, Yamato M, Nishida K, Yang J, Tano Y, Okano T. Limbal epithelial side-population cells have stem cell-like properties, including quiescent state. Stem Cells. 2006; 24:86–94. [PubMed: 16150918]
36. Mills AA, Zheng B, Wang X-J, Vogel H, Roop DR, Bradley A. p63 is a p53 homologue required for limb and epidermal morphogenesis. Nature. 1999; 398:708–713. [PubMed: 10227293]
37. Joseph A, Powell-Richards AO, Shanmuganathan VA, Dua HS. Epithelial cell characteristics of cultured human limbal explants. Br J Ophthalmol. 2004; 88:393–398. [PubMed: 14977776]
38. Zhou S, Schuetz JD, Bunting KD, Colapietro AM, Sampath J, Morris JJ, Lagutina I, Grosveld GC, Osawa M, Nakauchi H, Sorrentino BP. The ABC transporter Bcrp1/ABCG2 is expressed in a wide variety of stem cells and is a molecular determinant of the side-population phenotype. Nat Med. 2001; 7:1028–1034. [PubMed: 11533706]
39. Du Y, Funderburgh ML, Mann MM, SundarRaj N, Funderburgh JL. Multipotent stem cells in human corneal stroma. Stem Cells. 2005; 23:1266–1275. [PubMed: 16051989]
40. Chen W, Hara K, Tian Q, Zhao K, Yoshitomi T. Existence of small slow-cycling Langerhans cells in the limbal basal epithelium that express ABCG2. Exp Eye Res. 2007 [Epub ahead of print].
41. Nakamura M, Okano H, Blendy JA, Montell C. Musashi, a neural RNA-binding protein required for Drosophila adult external sensory organ development. Neuron. 1994; 13:67–81. [PubMed: 8043282]

42. Kaneko Y, Sakakibara S, Imai T, Suzuki A, Nakamura Y, Sawamoto K, Ogawa Y, Toyama Y, Miyata T, Okano H. Musashi1: an evolutionally conserved marker for CNS progenitor cells including neural stem cells. Dev Neurosci. 2000; 22:139–153. [PubMed: 10657706]

43. Sakakibara S, Nakamura Y, Yoshida T, Shibata S, Koike M, Takano H, Ueda S, Uchiyama Y, Noda T, Okano H. RNA-binding protein Musashi family: roles for CNS stem cells and a subpopulation of ependymal cells revealed by targeted disruption and antisense ablation. Proc Natl Acad Sci U S A. 2002; 99:15194–15199. [PubMed: 12407178]

44. Jang YK, Jung DH, Jung MH, Kim DH, Yoo KH, Sung KW, Koo HH, Oh W, Yang YS, Yang SE. Mesenchymal stem cells feeder layer from human umbilical cord blood for ex vivo expanded growth and proliferation of hematopoietic progenitor cells. Ann Hematol. 2006; 85:212–225. [PubMed: 16391912]

45. Lee JB, Song JM, Lee JE, Park JH, Kim SJ, Kang SM, Kwon JN, Kim MK, Roh SI, Yoon HS. Available human feeder cells for the maintenance of human embryonic stem cells. Reproduction. 2004; 128:727–735. [PubMed: 15579590]

46. Stojkovic P, Lako M, Stewart R, Przyborski S, Armstrong L, Evans J, Murdoch A, Strachan T, Stojkovic M. An autogeneic feeder cell system that efficiently supports growth of undifferentiated human embryonic stem cells. Stem Cells. 2005; 23:306–314. [PubMed: 15749925]

47. Schramek H, Feifel E, Healy E, Pollack V. Constitutively active mutant of the mitogen-activated protein kinase kinase MEK1 induces epithelial dedifferentiation and growth inhibition in madin-darby canine kidney-C7 cells. J Biol Chem. 1997; 272:11426–11433. [PubMed: 9111053]

48. Fliniaux I, Viallet JP, Dhouailly D, Jahoda CA. Transformation of amnion epithelium into skin and hair follicles. Differentiation. 2004; 72:558–565. [PubMed: 15617566]

49. Uchida S, Suzuki Y, Araie M, Kashiwagi K, Otori Y, Sakuragawa N. Factors secreted by human amniotic epithelial cells promote the survival of rat retinal ganglion cells. Neurosci Lett. 2003; 341:1–4. [PubMed: 12676329]

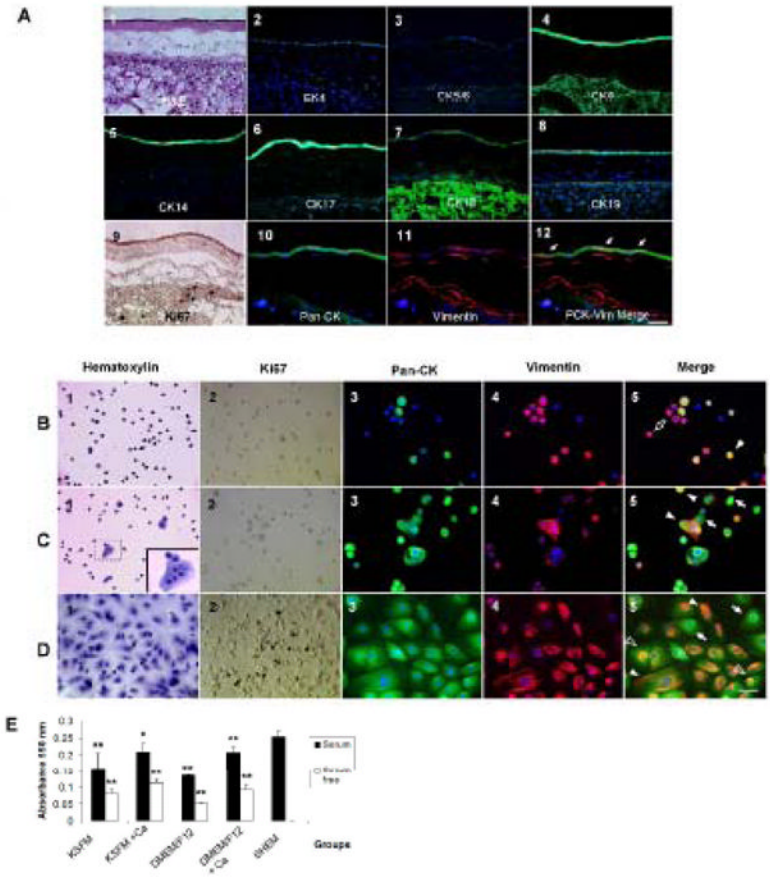

Figure 1. HAEC Phenotype *In Vivo* and *In Vitro*

(**A1**): Light micrograph with Hematoxylin & Eosin staining. (**A2–8**): Immunofluorescence staining of the CK (green) profile in HAECs and nuclear counterstaining (blue) with Hoechst 33342. (**A9**): Immunohistochemistry of Ki67 expression (brown) to indicate the cellular proliferation state. (**A10**): Epithelial marker using pan-CK (AE1/AE3) staining. (**A11**): Mesenchymal marker using Vim staining (Texas Red). (**A12**): A merged picture to show the colocalization of Pan-CK and Vim expressions. Arrows indicate co-expression (yellow) of these two markers. The scale bar represents 50 μm. Characterization of the HAEC Phenotype *In Vitro* (B–D). (**B**): serum-free and calcium-free/low culture media. (**C**): serum-free and high-calcium culture media. (**D**): serum-containing and high-calcium culture media. (**B1, C1, D1**): Representative light micrographs with Hematoxylin staining. Cell-cell contacts are observed in serum-free high calcium and serum-containing media. (**B2, C2, D2**): Immunohistochemistry of proliferative marker Ki67 (brown). (**B3, C3, D3**): Immunofluorescence staining of the epithelial marker pan-cytokeratin (green) with nuclear counterstaining (blue) with Hoechst 33342. (**B4, C4, D4**): Immunofluorescence staining of the mesenchymal marker Vim (red) with nuclear counterstaining (blue) with Hoechst 33342. (**B5, C5, D5**): Merged pictures to show colocalization of pan-CK and Vim expressions. Asterisks indicate negative staining to both markers (blue); arrows indicate positive staining to pan-CK only (green); open arrows indicate positive staining to Vim only (red); arrow heads indicate double positive staining to both markers (yellow); open arrow heads indicate a perinuclear scaffold of vimentin expression in pan-CK positive cells. The scale bar represents 50 μm. (**E**) MTT proliferative assay to compare the growth capacity of HAECs in all experimental conditions. *$p < 0.05$ and **$p < 0.01$, n=5, conditions versus SHEM medium.

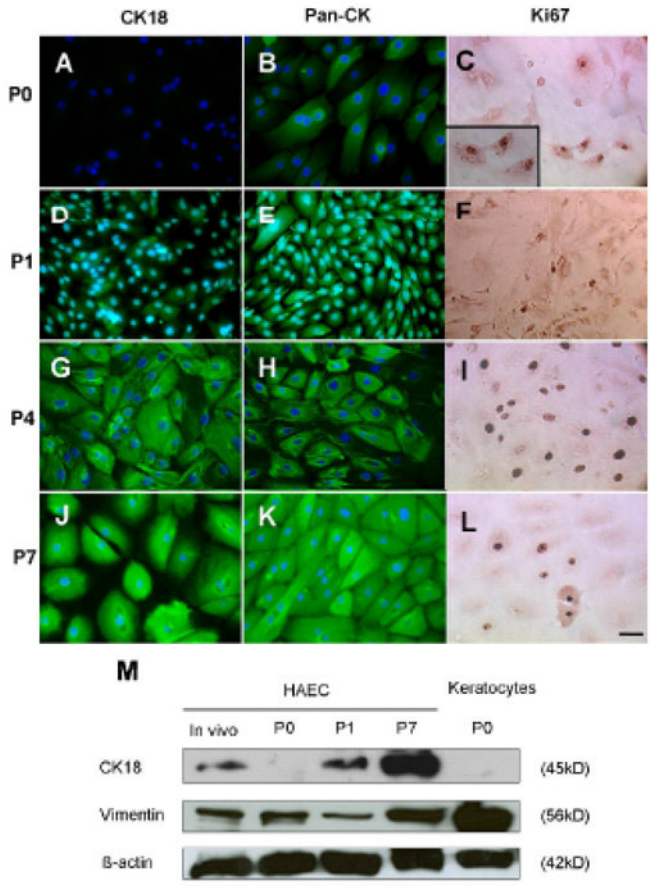

Figure 2. Cytokeratin and Proliferation Profiles of HAECs in SEHM at Different Passages

(**A, D, G, J**): Immunofluorescence staining to CK18 (green) with blue nuclear counterstaining with Hoechst 33342. (**B, E, H, K**): Immunofluorescence staining to the epithelial phenotypic marker, Pan-CK, (green) with nuclear counterstaining in blue. (**C, F, I, L**): Immunohistochemistry to Ki67 as an index of cell proliferation (brown nuclear staining). The scale bar represents 50 μm. (**M**) Representative western blotting profile of CK18 and Vim. Freshly isolated HAECs from the *in vivo* tissue were used as a baseline control for the comparison of HAECs cultured in SHEM from P0, P1 and P7. Corneal stromal keratocytes were used as a positive control for Vim blotting.

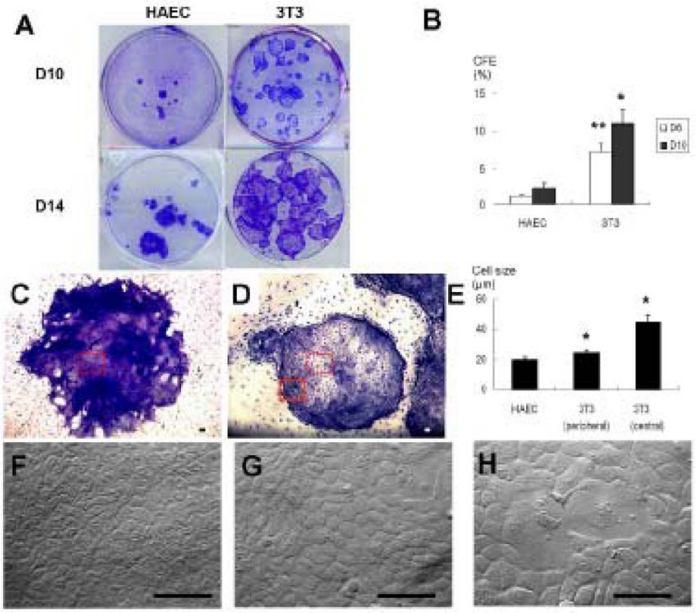

Figure 3. Comparison of Cell Size and Morphology of Limbal Clones

(**A**): Representative cultures of limbal clones on HAEC and 3T3 feeder layers at Day 10 and Day 14. (**B**): Colony-forming efficiency of limbal clones on HAEC and 3T3 feeder layers at Day 6 and Day 10 (*$p < 0.05$ and **$p < 0.01$, 3T3 versus HAEC, n=3). (**C, D**): Epithelial morphology of a representative limbal clone on HAEC or 3T3 feeder layers at a low magnification (40 x). The scale bar represents 100 μm. (**E**): The average cell size of limbal clones on HAEC feeder layers, at the periphery and the center of limbal clones on 3T3 feeder layers (* each $p < 0.05$, 3T3 versus HAEC, n=3). (**F**): Epithelial cell morphology in the limbal clone (from the dotted square in **C**) on HAEC feeder layers at a high magnification (400x). (**G**): Epithelial cell morphology in the periphery (from the square outlined in **D**) on a 3T3 feeder layers. (**H**): A heterogeneous cell size was noted in the center of limbal clones (from the dotted square in **D**) on 3T3 feeder layers. The scale bar represents 100 μm.

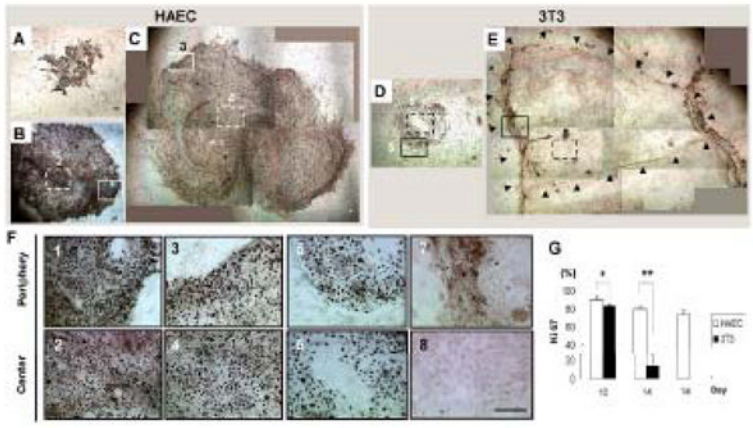

Figure 4. Comparison of Cell Proliferation in Limbal Clones

(**A**–**E**): Immunofluorescence staining to cell proliferation marker Ki67 (brown) in limbal clones supported on HAEC or 3T3 feeder layers at lower magnification (40x). (**F**): Higher magnification of outlined areas numerated from 1 to 8 in B–E (200x). Time points included D10 (**A, D**), D14 (**B, F**) and D18 (**C**). Black arrows in Figure E indicate the margin of a subconfluen 3T3-supported limbal clone. Open arrow heads in Figure F6 indicate cell nuclei stained negative to Ki67. (**G**): The percentage of Ki67-positive cells in HAEC- or 3T3-supported clones was significantly different (*$p < 0.05$, n=3; **$p < 0.01$, n=3). The scale bar represents 100 μm.

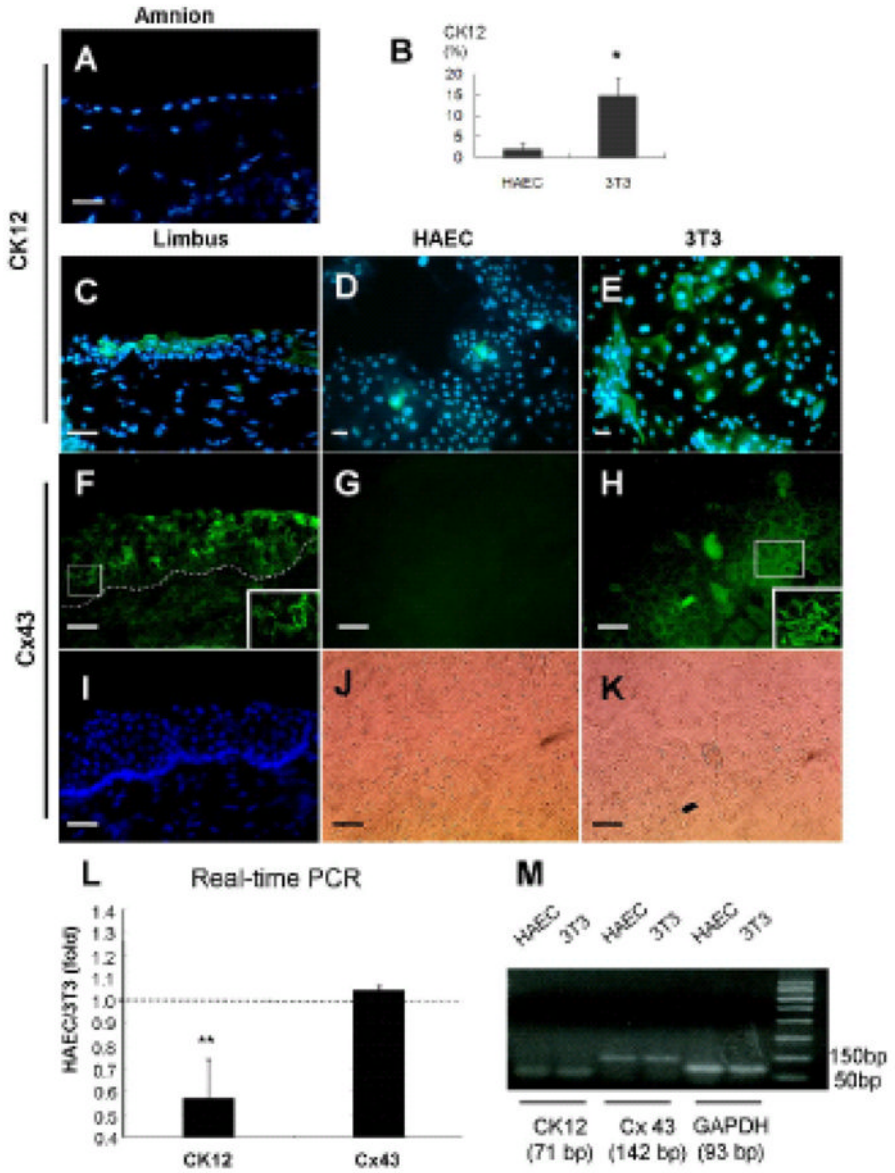

Figure 5. Comparison of CK12 and Connexin 43 Expressions

(**A**): Immunofluorescence staining to CK12 (green) in a fresh amnion tissue. (**B**): The percentage of CK12-expressing cells in limbal clones cultured on HAEC or 3T3 feeder layers (*$p < 0.05$, n=3). (**C, D, E**): Immunofluorescence staining to CK12 (green) in a fresh limbal tissue, limbal clones on HAEC and 3T3 feeder layers, respectively. (**F–H**): Immunofluorescence staining to connexin 43 (green) in a fresh limbal tissue, limbal clones on HAEC and 3T3 feeder layers, respectively. Limbal suprabasal layers showed positive intercellular staining to connexin 43. Insets from the outlined squares in **F** and **H** clearly demonstrated a punctate staining pattern. (**I**): Nuclear counterstaining showed negative limbal basal cells and the location of basement membrane. (**J, K**): Phase micrographs of limbal clones in **G** and **H**, respectively. The scale bar represents 50 μm. (**L**): A representative real-time PCR analysis showed a significant difference of CK12 (** $p < 0.01$, compared to 1-fold, n=3), but not connexin 43, in the transcript expression between HAEC-supported and 3T3-supported clones (The dotted line indicates 1 fold) (**M**): DNA

electrophoretic analysis verified the end-product of real-time PCR. GAPDH was used as an internal control.

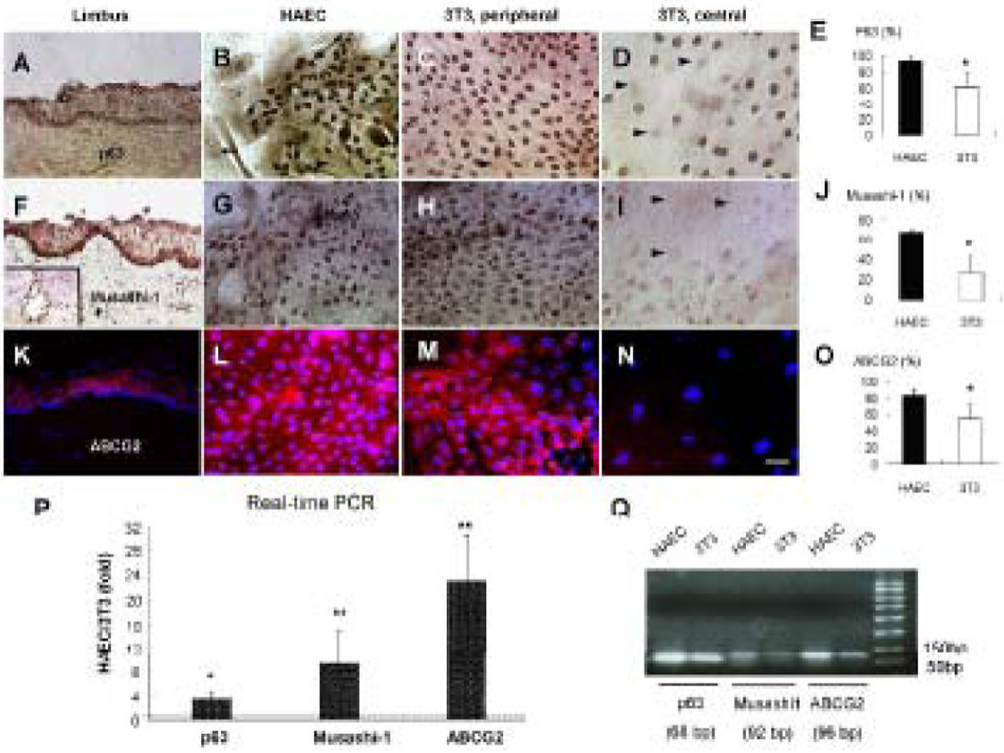

Figure 6. Comparison of p63, Musashi-1 and ABCG2 Expression

(**A–D**): Nuclear expression of p63 (brown) is positive in limbal basal epithelial cells *in vivo* (**A**), in nearly all cells in HAEC-supported limbal clones (**B**), and in the majority of clonal cells in the periphery (**C**) but not in large cells of the center of 3T3-supported limbal clones (**D**). Arrow heads indicate negative staining to p63. (**F–I**): Nuclear expression to Musashi-1 (brown) is mainly in the limbal basal layer *in vivo* (**F**), evenly distributed in nearly all cells in HAEC-supported limbal clones (**G**), and in the periphery (**H**) but much less in the center of 3T3-supported limbal clones (**I**). The inset in **F** shows a positive control of Musashi-1 staining in the subventricular neural progenitors of a mouse brain. Arrow heads in **I** indicate negative staining to Musashi-1 in large cells. (**K–N**): Membrane expression to ABCG2 (red) is observed mainly in limbal basal epithelium (**K**), nearly all cells in HAEC-supported limbal clones (**L**), and patches of small cells in the periphery (**M**), but not in large cells in the center of 3T3-supported limbal clones (**N**). The scale bar represents 50 μm. (**E, J, O**): Percentages of p63-, Musashi-1-, or ABCG2-positive cells in limbal clones on HAEC or 3T3 feeder layers, respectively (*$p < 0.05$, n=4). (**P**): Real-time PCR for p63, Musashi-1, and ABCG2 expressions by limbal clones cultured on HAEC and 3T3 feeder layers. A representative case is taken from 3 separate donor limbal tissues corneas with similar results. Transcript levels of each gene in limbal clones are shown as relative folds of HAEC versus 3T3. A dotted line indicates 1 fold. (* $p < 0.05$, ** $p < 0.01$, compared to 1-fold, n=3) (**Q**): DNA electrophoretic analysis of end-product of real-time PCR showed expected sizes of amplicons.

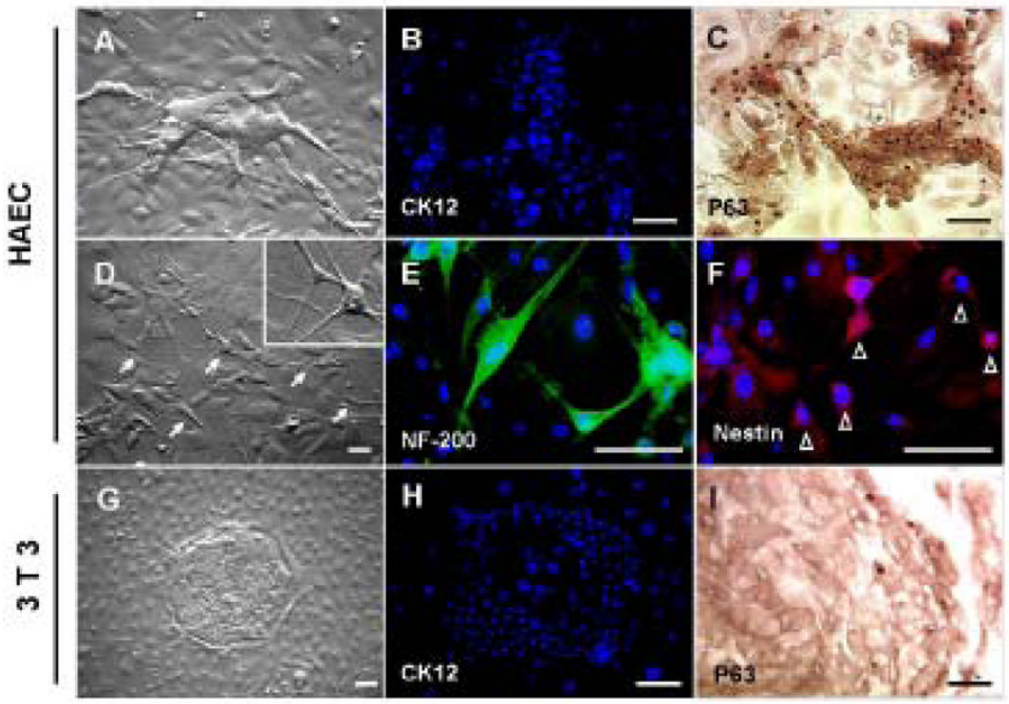

Figure 7. Characterization of Limbal Clones Subcultured on HAEC Feeder Layers

(A): Daughter epithelial clones from the primary limbal epithelial clones cultured on HAEC feeders. These clones showed negative staining to CK12 (green, **B**), but positive staining to p63 (brown, **C**) on D14. Furthermore, they also generated daughter clones containing dendritic neurons (arrows) **(D)**. Inset: a high magnification of the neuron-like cells indicated by arrows. Among them, dendritic cells were positively stained to neurofilament 200 (green, **E**) in the elongated dendritic cytoplasmic processes, while some smaller and less dendritic cells expressed nestin (red, **F**), casting a perinuclear filamentous “nest” (open arrow heads), in contrast to a blue nuclear counterstaining by Hoechst 33342. **(G):** Primary limbal clones on 3T3 feeder layers only gave rise to epithelial daughter clones. These clones showed negative staining to CK12 (green, **H**) and minimal positive staining to p63 only in the periphery of the clone (brown, **I**) on Day 14. The scale bar represents 50 μm.

Table 1

Culture Materials.

Material	Source	Concentration
Cell culture dishes, plates and centrifuge tubes	Becton Dickinson (Franklin Lakes, NJ)	-
Dulbecco's modified Eagle's medium (DMEM)	Gibco-BRL (Grand Island, NY)	[Ca2+]=1.8 mM
F-12 nutrient mixture (F12)	Gibco-BRL (Grand Island, NY)	[Ca2+]=0.299 mM
Fetal bovine serum (FBS)	Gibco-BRL (Grand Island, NY)	100%
Hank's balanced salt solutions (HBSS)	Gibco-BRL (Grand Island, NY)	-
Amphotericin B, Gentamycin	Gibco-BRL (Grand Island, NY)	-
Keratinocyte serum-free medium with supplement (KSFM), defined	Gibco-BRL (Grand Island, NY)	[Ca2+] = 0.07 mM
Trypsin/EDTA	Gibco-BRL (Grand Island, NY)	0.25%/1 mM
Calcium-free DMEM/F-12 mixture	Sigma-Aldrich (St. Louis, MO)	[Ca2+] = 0 mM
Cholera toxin	Sigma-Aldrich (St. Louis, MO)	-
Dimethyl sulfoxide	Sigma-Aldrich (St. Louis, MO)	-
Hydrocortisone	Sigma-Aldrich (St. Louis, MO)	-
Insulin-transferrin-sodium selenite media supplement	Sigma-Aldrich (St. Louis, MO)	-
mouse-derived epidermal growth factor (EGF)	Sigma-Aldrich (St. Louis, MO)	-
Supplemented hormonal epithelial medium (SHEM)	Customized mixture	[Ca2+]=1.05 mM
		HEPES-buffered DMEM/F12 (50%/50%)
		0.5% dimethyl sulfoxide
		10 ng/ml EGF
		5 μg/ml insulin
		5 μg/ml transferring
		5 ng/ml sodium selenite
		0.5 μg/ml hydrocortisone
		10-10 M cholera toxin
		5% FBS
		50 μg/ml gentamicin
		1.25 μg/ml amphotericin B.
Calcium chloride	Fluka (Steinheim, Switzerland)	1 M
Mitomycin C	Roche (Indianapolis, IN)	-
Dispase II powder	Roche (Indianapolis, IN)	

Table 2

Antibodies Used for Immunofluorescence Staining, Immunohistochemistry and Western Blotting.

Antibody (Host/Type)	Clone	Source	Titration
CK4 (Ms/Mono)	6B10	Sigma (St. Louis, MO)	1:200 (IF)
CK5/6 (Ms/Mono)	-	Santa Cruz Biotechnology (Santa Cruz, CA)	1:100 (IF)
CK8 (Ms/Mono)	C51	ICN Biomedicals (Irvine, CA)	1:100 (IF)
CK12 (Gt/Poly)	-	Santa Cruz Biotechnology, (Santa Cruz, CA)	1:200 (IF)
CK14 (Ms/Mono)	RCK107	Chemicon (Temecula, CA)	1:100 (IF)
CK17 (Ms/Mono)	CK-E3	Sigma (St. Louis, MO)	1:300 (IF)
CK18 (Ms/Mono)	DC10	DakoCytomation, (Carpinteria, CA)	1:50 (IF) 1:500 (WB)
CK19 (Ms/Mono)	RCK108	DakoCytomation, (Carpinteria, CA)	1:100 (IF)
Pan-cytokeratin (Ms/Mono)	AE1/AE3	DakoCytomation, (Carpinteria, CA)	1:50 (IF)
Ki67 (Ms/Mono)	MIB-1	DakoCytomation, (Carpinteria, CA)	1:100 (IHC)
p63 (Ms/Mono)	4A4	DakoCytomation, (Carpinteria, CA)	1:50 (IHC)
ABCG2 (Ms/Mono)	BXP-21	Chemicon (Temecula, CA)	1:25 (IF)
Vimentin (Rb/Poly)	-	Abcam (Cambridge, MA)	1:100 (IF) 1:500 (WB)
Musashi-1 (Rb/Poly)	-	Abcam (Cambridge, MA)	1:100 (IHC)
Connexin 43 (Rb/Poly)	-	Zymed (San Francisco, CA)	1:50 (IF)
ABC kit	-	Vectastain Elite, Vector Labs (Burlingame, CA)	-
DAB kit	-	DakoCytomation (Carpinteria, CA)	-

Abbreviations: Gt, goat-anti-human; IHC, immunohistochemistry; IF, Immunofluorescence; Ms, mouse-anti-human; Mono, monoclonal; Poly, polyclonal; Rb, rabbit-anti-human; WB, western blotting

Table 3

Culture Media Used in HAEC Cultures.

Condition #	**1**	**2**	**3**	**4**	**5**	**6**	**7**	**8**	**9**
Medium	KSFM	KSFM	KSFM	KSFM	DMEM/F12	DMEM/F12	DMEM/F12	DMEM/F12	SHEM
$[Ca^{++}]$ in mM	0.07	1.05	0.07	1.05	0	1.05	0	1.05	1.05
FBS	0	0	10%	10%	0	0	10%	10%	5%
Supplements	+	+	+	+	−	−	−	−	+

Abbreviations: DMEM/F12, Dulbecco's modified Eagle's medium/F-12 nutrient mixture mixed at an equal volume; FBS, fetal bovine serum; HAEC, human amniotic epithelial cells; KSFM, defined keratinocyte serum free medium; SHEM, supplemented hormonal epithelial medium

Table 4

Assay ID and Probe Sequences Used for Real-time PCR

Gene	Assay ID (TagMan Gene Expression Assays)	UniGene ID	Exon Boundary	Amplicon length	Probe sequence
glyceraldehyde- 3-phosphate dehydrogenase (GAPDH)	Hs02758891_g1	Hs.479728	7–8	93	GACTCATGA CCACAGTCC ATGCCAT
p63	Hs00978344_m1	Hs.137569	8–9	68	CGAAGCGCC CGTTTCGTC AGAACAC
Mushashil	Hs00159291_m1	Hs. 158311	11–12	92	AGCTTACAG CCATTCCTCT CACTGC
ABCG2	Hs01053796_m1	Hs.480218	9–10	96	CAGGCCTCTA TAGCTCAGAT CATTG
CK12	Hs01057907_m1	Hs.66739	7–8	71	TTCCTCTAAA GACCCAACC AAAACC
Connexin 43	Hs00748445_s1	Hs.74471	2-2	142	CAGTGGTGC GCTGAGCCC TGCCAAA